

Alcohol dehydrogenase coexisted solid-state electrochemiluminescence biosensor for detection of p53 gene

Wang Xiaoying¹ Wang Xiaoning² Zhang Xiangyi¹ Chen Fentian¹
Zhu Kehui¹ Yang Ligang¹ Tang Meng¹

(¹Key Laboratory of Environmental Medicine and Engineering of Ministry of Education, Southeast University, Nanjing 210009, China)

(²Department of Hematology, the First Affiliated Hospital of Xi'an Jiaotong University, Xi'an 710061, China)

Abstract: An alcohol dehydrogenase (ADH)-coexisted solid-state electrochemiluminescence (ECL) biosensor for sensitive detection of the p53 gene was developed. The electrode modified by multiwalled carbon nanotubes, $\text{Ru}(\text{bpy})_3^{2+}$ and polypyrrole (MWNTs-Ru(bpy)₃²⁺-PPy) was prepared to adsorb the ssDNA by electrostatic interactions. Then, the ssDNA recognized the gold nanoparticles (AuNPs)-labeled p53 gene and produced the AuNPs-dsDNA electrode with the AuNPs layer. The AuNPs layer adsorbed the ADH molecules for producing the ECL signal. Thus, the biosensor was based on coupling enzyme substrate reaction with solid-state ECL detection, and it displayed good sensitivity and specificity. The detection limit of the wild type p53 sequence (wtp53) is as low as 0.1 pmol/L and the discrimination is up to 57.1% between the wtp53 and the muted type p53 sequence (mtp53). The amenability of this method to the analyses of p53 from normal and cancer cell lysates is demonstrated. The signal of wtp53 in the MGC-803 gastric cancer cell lysates turns out to be about 61.8% that of the wtp53 in the GES-1 normal gastric mucosal cell lysates, and the concentration of the wtp53 is found to decrease about 59 times. The method is highly complementary to enzyme-linked immunosorbent assay (ELISA), and it holds promise for the diagnosis and management of cancer.

Key words: MWNTs-Ru(bpy)₃²⁺ composite; solid-state electrochemiluminescence; alcohol dehydrogenase; wild type p53 sequence; muted type p53 sequence; cell lysates

doi: 10.3969/j.issn.1003-7985.2013.02.007

The p53 gene is located on chromosome 17 p13. It contains 11 exons spanning 20 kilobases and encodes

a (mostly) nuclear phosphoprotein of 53 kD. This gene belongs to a family of highly conserved genes that contains at least two other members, P63 and P73. However, P53 appears to differ from its cousins by its unique role in tumor suppression. About 50% of all the malignancies contain a mutation in p53 and aggressive growth of several types of cancer has been attributed to mutations in this gene. Moreover, p53 is also involved in sustaining cellular homeostasis and in complex regulatory interactions^[1-2]. Sequence-specific analysis of the p53 gene can help early diagnosis of cancer development and consequently increase the success of the treatment^[3-4]. Therefore, the specific recognition and quantitative detection of the p53 gene and the mutations in the p53 gene are extremely crucial in fundamental research as well as in clinical practice.

So far, a variety of methods for measuring the p53 gene have been reported. Among traditional methods for molecular diagnosis and also for p53, the distinction is made between point mutation scanning and screening technologies. Scanning technologies aim at finding unknown mutations in candidate or known disease genes, such as direct DNA sequencing. Screening techniques with high throughput^[5], such as denaturing high-performance liquid chromatography (DHPLC)^[6], single-strand conformation polymorphism (SSCP)^[7], and denaturing gradient gel electrophoresis (DGGE)^[8], aim at finding known mutations. However, some of these approaches are time-consuming and require highly skilled labor, while others are less sensitive or more expensive in equipment use. In recent years, a new trend for the detection of p53 mutations has turned to high-sensitivity and specificity, real-time and rapid detection. Biosensors, in particular DNA-based sensors, are of considerable recent interest due to their tremendous promise for obtaining sequence-specific information in a faster, simpler and cheaper manner compared with traditional hybridization assays. Different transduction principles have been employed for p53 DNA detection including electrochemical^[9-13], piezoelectric^[14-15] and optical techniques^[16-18].

Recently, we develop a glucose-dehydrogenase (GDH)-based solid-state electrochemiluminescence (ECL) biosensor for sensitive detection of a single point mutation in the p53 gene^[19]. In the strategy, we try to

Received 2012-11-20.

Biography: Wang Xiaoying (1980—), female, doctor, lecturer, wxy@seu.edu.cn.

Foundation items: The National Basic Research Program of China (973 Program) (No. 2010CB732404, 2011CB933404), the National Natural Science Foundation of China (No. 81172697, 81170492, 81001244), the Specialized Research Fund for the Doctoral Program of Higher Education (No. 20110092120055), the Foundation of the State Key Laboratory of Bioelectronics of Southeast University.

Citation: Wang Xiaoying, Wang Xiaoning, Zhang Xiangyi, et al. Alcohol dehydrogenase coexisted solid-state electrochemiluminescence biosensor for detection of p53 gene[J]. Journal of Southeast University (English Edition), 2013, 29(2): 145 – 151. [doi: 10.3969/j.issn.1003-7985.2013.02.007]

combine the high sensitive solid-state ECL technique with the selectivity of the enzyme biosensor together. The biosensor displays good sensitivity, specificity and a high degree of discrimination between the wild type p53 sequence (wtp53) and the muted type p53 sequence (mtp53). But the detection conditions of the biosensor are complex and the stability is poor. Herein, a few minor adjustments have been made for the sensing system. The composite of MWNTs-Ru(bpy)₃²⁺ is prepared and coated on a glassy carbon (GC) electrode through hydrophobic interaction instead of a gold electrode. The MWNTs-Ru(bpy)₃²⁺ composite on the GC electrode has better stability. The alcohol dehydrogenase (ADH) substitution for the GDH can simplify the composition of the detecting solution. The amenability of this method to the analyses of p53 from the GES-1 normal gastric mucosal cell lysates and the MGC-803 gastric cancer cell lysates is demonstrated.

1 Materials and Methods

1.1 Reagents and apparatus

Oligonucleotides were purchased from Shengggong Bio-engineering Ltd Company (Shanghai, China). The sequence of wide type p53 (wtp53) is 5'-HS-(CH₂)₆-GGCACAAACACGCACCTCAA-3'; the sequence of muted type p53 (mtp53) is 5'-HS-(CH₂)₆-GGCACAAA-CATGCACCTC AA-3'; the complementary sequence of the wtp53 (ssDNA) is 5'-(CH₂)₆-TTGAGGTGCGT-GTTTGTGCC-3'; the three-base mismatched sequence of the wtp53 is 5'-HS-(CH₂)₆-GGCCCCAAACAAGCAC CGCAA-3' (Italic nucleotides are the mismatched bases). Ru(bpy)₃²⁺ (99.95%), HAuCl₄, Pyrrole monomer (> 99%), 1-ethyl-3-[(3-dimethylamino) propyl] carbodiimide (EDC), nicotinamide adenine dinucleotide (NAD⁺, sodium salt, from yeast), ethanol and alcohol dehydrogenase (ADH) were purchased from Sigma (USA). GES-1 normal gastric mucosal cells and MGC-803 gastric cancer cells were purchased from Shanghai Institute of Life Science Cell Resource Center (Shanghai, China). Multiwalled carbon nanotubes (40 to 60 nm in diameter, 1 to 10 μm in length) functionalized with the carboxylic

group (COOH-MWNTs) were obtained from Shenzhen Nanotech Port Co., Ltd. (Shenzhen, China). 10 mmol/L PBS (pH 7.3) and 10 mmol/L PBS containing 0.5 mol/L NaCl (pH 7.3) were used for hybridization reaction. 10 mmol/L PBS containing 137 mmol/L NaCl, 2.7 mmol/L KCl (pH 7.4) and 50 mmol/L Tris-HCl containing 150 mmol/L NaCl, 0.02% NaN₃, 0.1% sodium dodecyl sulfate (SDS), 100 μg/mL phenylmethanesulfonyl fluoride (PMSF), 1 μg/mL aprotinin, 1% Triton X-100 and 0.5% sodium deoxycholate (pH 8.0) were used as the cell lysis buffer. 20 mmol/L PBS containing 300 μmol/L alcohol and 1.0 mmol/L NAD⁺ (pH 7.5) were used as the detecting solution. Other reagents were of analytical reagent grade. All the solutions were prepared with ultrapure water from a Millipore Milli-Q system.

ECL was recorded with a MPI-E electrogenerated chemiluminescence analyzer (Xi'an Remax Electronic Science-Tech Co., Ltd., China), and a CHI 660A electrochemical analyzer (CHI instruments Inc., USA) was used to measure impedance and cyclic voltammogram (CV) in a 10 mL analytical cell.

1.2 Fabrication of ADH coexisted solid-state ECL biosensor

The schematic diagram of the ADH coexisting solid-state ECL biosensor for the detection of single nucleotide mutation in a p53 gene is shown in Fig. 1. The following is the detailed preparation processes. The MWNTs-Ru(bpy)₃²⁺ composite was prepared as previously described^[19]. The surface of GC electrode was carefully polished with 0.3 μm Al₂O₃ powders successively, rinsed with water and ethanol in an ultrasonic bath briefly and then allowed to dry at room temperature. 2 μL aliquot of the suspension of MWNTs-Ru(bpy)₃²⁺ composite was placed on the GC electrode surface and air-dried at room temperature. Then, the electrode was dipped into a 0.05 mol/L pyrrole aqueous solution containing 0.1 mol/L KCl-HCl (pH 3.0) to carry out cyclic voltammetry between 0 and +0.7 V (vs. Ag/AgCl) for 16 cycles with a scan rate of 50 mV/s. Thus, the MWNTs-Ru(bpy)₃²⁺-PPy was formed on the GC electrode surface.

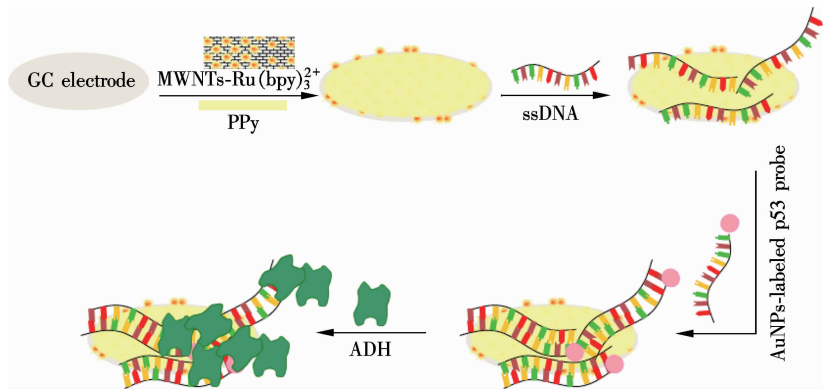


Fig. 1 Schematic representation of the preparation of ADH-coexisted solid-state ECL biosensor for detection of p53 sequences

The MWNTs-Ru(bpy)₃²⁺-PPy electrode was immersed into a 0.1 mol/L acetate buffer solution (pH 5.4) containing ssDNA, while applying a constant potential at +0.5 V (vs. Ag/AgCl) for 300 s. Then the electrode was rinsed with 10 mmol/L PBS (pH 7.3), and the ssDNA electrode was formed.

The ssDNA electrode was immersed into 10 mmol/L PBS (pH 7.3) containing 0.5 mol/L NaCl and AuNPs-labeled p53 probe (AuNPs-labeled p53 probe was prepared according to Ref. [19]), and a constant potential at +0.5 V (vs. Ag/AgCl) was applied for 300 s. Then the electrode was washed thoroughly with 10 mmol/L PBS (pH 7.3) to remove the unhybridized probe. The AuNPs-dsDNA electrode was obtained.

The AuNPs-dsDNA electrode was incubated with ADH in 10 mmol/L PBS (pH 7.3) at 4 °C for 12 h to attach ADH onto AuNPs. Then the electrode was washed with the same buffer thoroughly. The ADH electrode was obtained and employed as working electrode to detect ECL signal.

1.3 Preparation of real sample

The soluble cell lysates of the GES-1 normal gastric mucosal cells and MGC-803 gastric cancer cells were prepared according to Makmura et al. [20]. The procedure is as follows: Cells were washed three times with ice-cold 10 mmol/L PBS containing 137 mmol/L NaCl and 2.7 mmol/L KCl (pH 7.4). After decanting the PBS solution, cells were lysed in 50 mmol/L Tris-HCl containing 150 mmol/L NaCl, 0.02% NaN₃, 0.1% sodium dodecyl sulfate (SDS), 100 µg/mL phenylmethanesulfonyl fluoride (PMSF), 1 µg/mL aprotinin, 1% Triton X-100 and 0.5% sodium deoxycholate (pH 8.0) on ice for 20 min. The lysed cells were then removed from the tube walls by a cell slicker and transferred to a centrifuge tube. After sonication for 30 s on ice, contents released from the cell were centrifuged at 4 °C at 12 000 r/min for 10 min. The supernatant was collected and mixed with a fresh AuNPs solution for 40 h at 4 °C. The mixtures were stored at 4 °C for later use.

1.4 ECL measurement

The ECL determinations were performed at room temperature in a 10 mL homemade quartz cell. A three-electrode system used in this study included the modified GC electrode (3 mm in diameter) as the working electrode, an Ag/AgCl (sat.) as the reference electrode and a platinum wire as the counter electrode. The cyclic voltammetry mode with continuous potential scanning from 0 to 1.2 V and the scanning rate of 0.1 V/s was applied to achieve the ECL signal in 20 mmol/L PBS containing 300 µmol/L alcohol and 1.0 mmol/L NAD⁺ (pH 7.5). Since NAD⁺ was unstable in a strongly alkaline solution^[21], pH 7.5 was used in all experiments. A high

voltage of −800 V was supplied to the photomultiplier for luminescence intensity determination. The ECL and CV curves were recorded simultaneously.

2 Results and Discussion

2.1 SEM images of COOH-MWNTs, MWNTs-Ru(bpy)₃²⁺ composite and MWNTs-Ru(bpy)₃²⁺-PPy electrode

Using the SEM, we analyzed the micro-morphology of COOH-MWNTs, MWNTs-Ru(bpy)₃²⁺ composite and MWNTs-Ru(bpy)₃²⁺-PPy modified GC electrode (see Fig. 2). The COOH-MWNTs were composed of a number of single MWNT as bundle aggregates, and these MWNT bundles wrap into a reticular structure (see Fig. 2(a)).

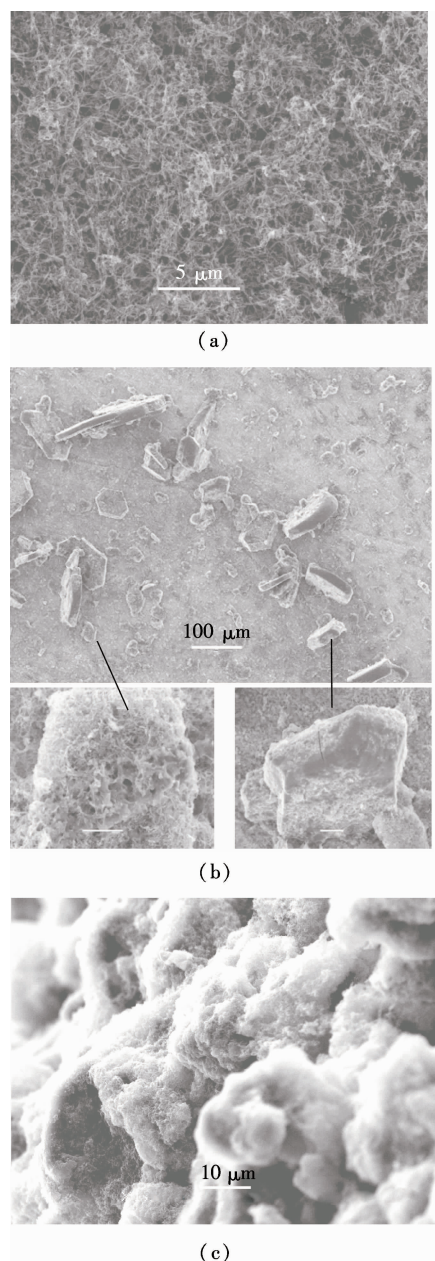


Fig. 2 SEM images. (a) COOH-MWNTs; (b) MWNTs-Ru(bpy)₃²⁺ composites; (c) MWNTs-Ru(bpy)₃²⁺-PPy electrode

Though MWNTs were very hydrophobic, COOH-MWNTs improved the solubility greatly. Negatively charged COOH-MWNTs, with a high specific surface area, immobilized stably a large number of positively charged $\text{Ru}(\text{bpy})_3^{2+}$ in the form of composites via electrostatic interaction. Many agglomerations can be seen in the composites (see Fig. 2(b)). As shown in Fig. 2(c), a three dimensional porous and dense modification layer on the electrode surface with positive charge was obtained for MWNTs- $\text{Ru}(\text{bpy})_3^{2+}$ -PPy modified GC electrode. In this case, COOH-MWNTs served as the nanosized backbone for PPy polymerization, with a result that the porous PPy film covered around the COOH-MWNTs in a cylinder structure. Finally, the electrochemical surface area for the MWNTs- $\text{Ru}(\text{bpy})_3^{2+}$ -PPy electrode was much larger than that for the bare GC electrode.

2.2 Characterization of ADH-coexisted solid-state ECL biosensor

The fabrication process of the ADH-coexisted solid-state ECL biosensor was characterized by electrochemical impedance spectroscopy (EIS) and cyclic voltammogram (CV). As shown in Fig. 3(a), the R_{et} for the bare GC electrode was 253.1 Ω (curve 1). Nevertheless, the R_{et} of the MWNTs- $\text{Ru}(\text{bpy})_3^{2+}$ electrode (curve 2) and the MWNTs- $\text{Ru}(\text{bpy})_3^{2+}$ -PPy electrode (curve 3) decreased dramatically, which were 17.2 and 14.7 Ω , respectively. This reflected the outstanding charge-transport characteristics of the MWNTs and PPy, which might greatly promote electron-transfer reactions of the electrode surface. Once the ssDNA was adsorbed onto the MWNTs- $\text{Ru}(\text{bpy})_3^{2+}$ -PPy electrode by electrostatic interactions, R_{et} increased to 489.6 Ω as shown in curve 4. It was due to the fact that the ssDNA, which had a single-strand nucleic acid with negative charges on its phosphate backbone, made an electrostatic repulsive force to $[\text{Fe}(\text{CN})_6]^{3-/4-}$. When the AuNPs-dsDNA electrode was formed, the increase in the amount of nucleic acid made a stronger repulsive force to $[\text{Fe}(\text{CN})_6]^{3-/4-}$. As a result, R_{et} was changed to 751.2 Ω (curve 5). Finally, the ADH was successfully absorbed into the AuNPs. R_{et} changed to 1 323.8 Ω (curve 6). This is probably attributable to the fact that the layer of enzyme molecules can insulate the conductive support and perturb the interfacial electron transfer between the redox couple $[\text{Fe}(\text{CN})_6]^{3-/4-}$ and the electrode^[22-23].

The corresponding CV curves of the electrodes with a scan rate of 0.1 V/s, and a scan range from -0.2 to 0.6 V are shown in Fig. 3(b). A symmetric and reversible voltammogram was obtained for a bare GC electrode (curve 1). Compared with the former, the voltammogram observed at the MWNTs- $\text{Ru}(\text{bpy})_3^{2+}$ electrode (curve 2) displayed a significant increase in the redox current. A further increase was presented in the redox

current for the MWNTs- $\text{Ru}(\text{bpy})_3^{2+}$ -PPy electrode (curve 3). It is attributable to the fact that MWNTs and PPy have a large specific surface area and outstanding charge-transport characteristics. Therefore, they greatly promote the interfacial electron transfer between the redox couple $[\text{Fe}(\text{CN})_6]^{3-/4-}$ and the electrode. Asymmetric and irreversible waves accompanied by a decline in the redox current were obtained for ssDNA electrode (curve 4), AuNPs-dsDNA electrode (curve 5) and ADH electrode (curve 6), respectively. The change in R_{et} and the CV curves of the electrodes illustrated the successful modification of the biosensing components on the GC electrode. It also indicated that the interactions between the MWNTs- $\text{Ru}(\text{bpy})_3^{2+}$ -PPy and the ssDNA, as well as the AuNPs and ADH rose successively.

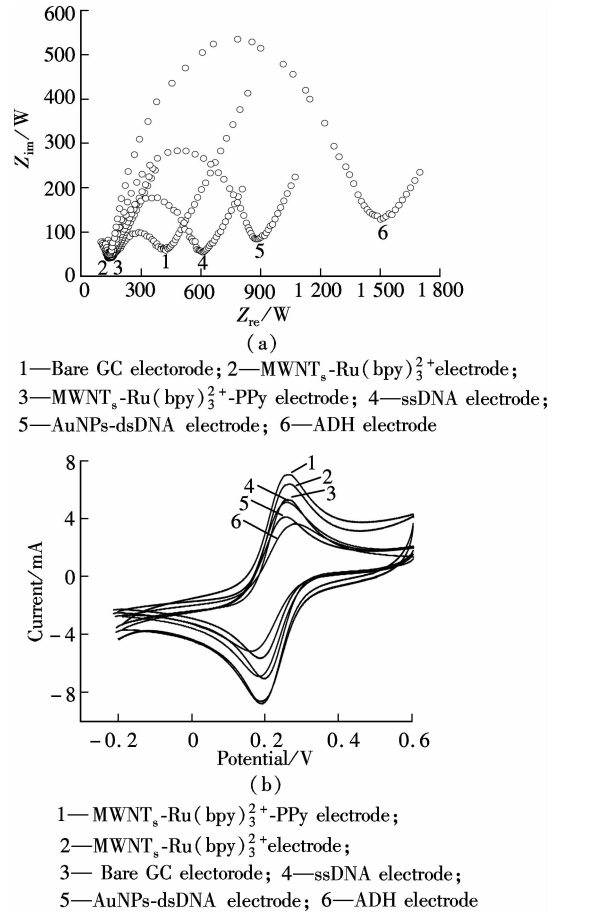


Fig. 3 The characterization of ADH-coexisted solid-state ECL biosensor. (a) Nyquist plots for the impedance measurement in 10 mmol/L $[\text{Fe}(\text{CN})_6]^{3-/4-}$ solution; (b) The corresponding cyclic voltammogram curves in 1 mmol/L $[\text{Fe}(\text{CN})_6]^{3-/4-}$ solution

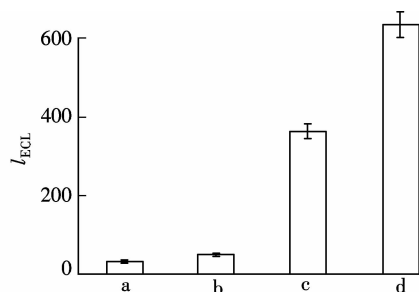
2.3 Optimization of experimental conditions

The detecting solution has a great impact on ECL intensity. The signal of the influence of NAD^+ concentration was investigated. In 20 mmol/L PBS (pH 7.5), with the concentration of NAD^+ increasing, the ECL intensity increased. When 1.5 mmol/L NAD^+ were added, the response reached the largest. As the concentration kept

increasing, the signal decreased slightly. The increased response may be explained by higher conversion efficiency with higher concentration of NAD^+ in the enzyme-catalyzed reaction. Considering the high cost of cofactor NAD^+ , 1.0 mmol/L NAD^+ was used in all other experiments. Furthermore, 20 mmol/L PBS (pH 7.5) containing 300 $\mu\text{mol/L}$ ethanol can provide stable ECL signal. Therefore, 20 mmol/L PBS containing 300 $\mu\text{mol/L}$ alcohol and 1.0 mmol/L NAD^+ (pH 7.5) was selected as the detecting solution.

2.4 Specificity, repeatability and stability of ADH-coexisted solid-state ECL biosensor

The MWNTs- $\text{Ru}(\text{bpy})_3^{2+}$ -PPy electrode not only immobilized stably a large number of $\text{Ru}(\text{bpy})_3^{2+}$ in the form of composites via electrostatic interaction (see Fig. 2), but also provided a stable modification layer for linking biomolecules and presented a large specific surface area and a good electronic transfer property. Thereby, it can dramatically increase the amount of ssDNA attachment, hybridization sensitivity and can provide an effective electronic tunnel for the combination of enzyme reaction and ECL reaction to some extent. Herein, the binding specificity of the ADH-coexisted solid-state ECL biosensor was investigated by the control hybridization experiments for wtp53, mtp53, three-base mismatched sequence of the wtp53 and blank. As shown in Fig. 4, only the wtp53 shows a maximal ECL intensity. The signal of the mtp53 (C/T mismatched) turns out to be about 57.1% that of the wtp53, when they are in the same concentration. In other words, the discrimination (The signal of the mismatched sequence reaches the percentage of the signal of the complementary sequence when they are in the same concentration) of wtp53 and mtp53 is 57.1%. The signal can be negligible for the three-base mismatched sequence of the wtp53 or blank. The consistent data was obtained when the experiment was repeated three times to observe its reproducibility. The solid-state ECL biosensor shows a good reproducibility with RSD 4.71%.



a—Blank; b—300 nmol/L three-base mismatched sequence of the wtp53; c—300 nmol/L mtp53; d—300 nmol/L wtp53

Fig. 4 ECL intensity of ssDNA electrodes hybridization with different sequences

The ECL intensity of the solid-state ECL biosensor is recorded under continuously cyclic potential scanning for

20 cycles in 20 mmol/L PBS containing 300 $\mu\text{mol/L}$ alcohol and 1.0 mmol/L NAD^+ (pH 7.5) at a scan rate of 0.1 V/s. There was no obvious change in the ECL signal. Even after hundreds of cycles, only a slight decrease in the ECL signal was observed, indicating the good stability of the ADH-coexisted solid-state ECL biosensor.

2.5 Calibration curve of wtp53 detection

The sensitivity of the solid-state ECL biosensor is investigated. Fig. 5 (a) shows the I_{ECL} (the difference of ECL intensity between the ADH electrode and AuNPs-dsDNA electrode) of the ADH electrodes under the conditions that different concentrations of AuNPs-labeled wtp53 interact with the ssDNA. I_{ECL} is grown when the AuNPs-labeled wtp53 concentration is increased. I_{ECL} is found to be linear with the logarithm of the wtp53 concentration in the range from 0.3 to 300 pmol/L (containing 0.3, 3, 30 and 300 pmol/L) in Fig. 5 (b). The equation for the resulting calibration plot is $y = 84.61gx + 90.1$ where x is the concentration of wtp53 and y is I_{ECL} ; the correlation coefficient is 0.9987, and a detection limit of 0.1 pmol/L is estimated by using 3σ , where σ is the relative standard deviation of a blank solution, and $n = 11$. Meanwhile, the signal of the mtp53 (C/T mismatched) turns out to be about 57.1% that of the wtp53 when they are in the same concentration (see Fig. 5 (b)). Therefore, the enzyme-based ECL sensing platform can recognize sequence-specific p53 sequences (wtp53 and mtp53) with a discrimination of up to 57.1%. The consistent data is obtained as shown in Fig. 5 (b) when the experiment is repeated three times.

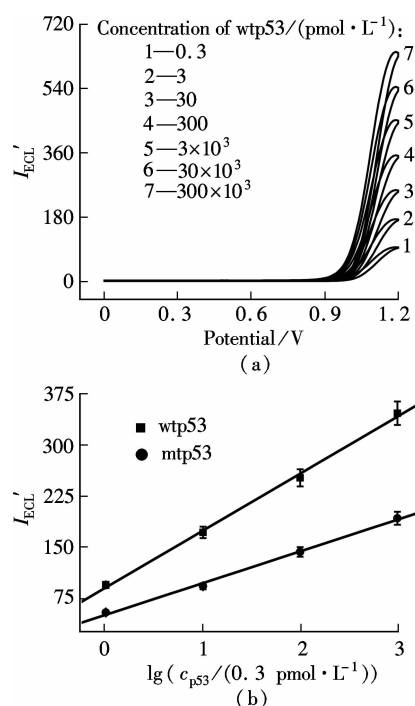


Fig. 5 Calibration curve of p53 detection. (a) ECL intensity-potential curves for the ADH electrodes with various wtp53 concentrations; (b) Calibration curves of p53 detection

2.6 Real sample analyses

Finally, we explored the feasibility of the method for real sample analyses. AuNPs were attached to the cysteine residues on the p53 molecules in the soluble cell lysates of the GES-1 normal gastric mucosal cells and the MGC-803 gastric cancer cells. Then, the ssDNA recognized the AuNPs-labeled p53 gene, and the AuNPs layer adsorbed the ADH molecules for producing the ECL signal. A well-defined ECL peak was observed when the ssDNA electrodes were used to capture wtp53 from the GES-1 normal gastric mucosal cell lysates. Meanwhile, the signal of the wtp53 in the MGC-803 gastric cancer cell lysates turns out to be about 61.8% that of the wtp53 in the GES-1 normal gastric mucosal cell lysates when they are in the same experimental conditions. To further establish the validity of this method for clinical applications, we conducted ELISA tests in parallel with this method for the analyses of the soluble cell lysates of the GES-1 normal gastric mucosal cells and the MGC-803 gastric cancer cells. As shown in Tab. 1, the significantly higher total p53 concentration in cancer cell lysates, determined by the ELISA test, is predominantly contributed by the elevation of the mutant p53. When compared with the results obtained with our method, it is clear that the elevation of the mutant p53 concentration is accompanied by a precipitous decline of the wtp53 concentration. Remarkably, the cancer cell assayed by our method displayed substantially (about 59 times, calculated according to the calibration curve of wtp53) lower wtp53 concentrations than that in the normal cell lysates, suggesting that the p53 gene had been severely mutated in these MGC-803 gastric cancer cells. These results were consistent with Ref. [12]. The consistent data was obtained when the experiment was repeated three times. The data in Tab. 1 demonstrate that our method is highly complementary to ELISA. The method is capable of determining p53 from real samples without extensive sample pretreatment/separation or specialized instruments and does not require the use of p53 antibodies. It holds promise as a clinical protocol for assaying p53 DNA binding capacity in normal and cancer cells at sensitive levels.

Tab. 1 Comparisons of total p53 and wtp53 concentrations between cancer and normal cell lysates nmol/L

Cell lysates	Total p53 (ELISA)	wtp53 (this method)
MGC-803 gastric cancer cells	1.3	0.009
GES-1 normal gastric mucosal cells	1.9	0.53

3 Conclusion

An ADH-coexisted solid-state ECL biosensor for the detection of a specific mutation in the p53 gene is designed. We explore the possibility of immobilizing en-

zymes and $\text{Ru}(\text{bpy})_3^{2+}$ on the same working electrode and combine the advantages of ECL detection and the selectivity of the enzyme biosensor. Consequently, the ADH-coexisted solid-state ECL biosensor displays a wide linear range, improved sensitivity and good stability. The assay allows detection at levels as low as 0.1 pmol/L of the wtp53, and the discrimination is up to 57.1% between the wtp53 and the mtp53. The sensor system is successfully applied to analyze wtp53 from the GES-1 normal gastric mucosal cell lysates and the MGC-803 gastric cancer cell lysates. The obtained results demonstrate that the ADH-coexisted solid-state ECL biosensor can distinguish sequences present in the various samples that differ only by one base; and, hence, it appears to be a candidate technique for the detection of gene mutation. Moreover, the successful demonstration of a diverse set of assay formats opens the door to ECL assays for a wide assortment of classical cancer clinical analytes.

References

- [1] Hofseth L J, Hussain S P, Harris C C. p53: 25 years after its discovery [J]. *Trends Pharmacol Sci*, 2004, **25** (4): 177–181.
- [2] Vousden K H, Lane D P. p53 in health and disease [J]. *Nat Rev Mol Cell Biol*, 2007, **8**(4): 275–283.
- [3] Hainaut P, Wiman K G. 30 years and a long way into p53 research [J]. *Lancet Oncol*, 2009, **10**(9): 913–919.
- [4] Olivier M, Hollstein M, Hainaut P. TP53 mutations in human cancers: origins, consequences, and clinical use [J]. *Cold Spring Harb Perspect Biol*, 2010, **2**(1): a001008-01–a001008-17.
- [5] Jiang T, Minunni M, Mascini M. Towards fast and inexpensive molecular diagnostic: the case of p53 [J]. *Clin Chim Acta*, 2004, **343**(1/2): 45–60.
- [6] Narayanaswami G, Taylor P D. Site-directed mutagenesis of exon 5 of p53: purification, analysis, and validation of amplicons for DHPLC [J]. *Genet Test*, 2002, **6**(3): 177–184.
- [7] Miyajima K, Tamiya S, Oda Y, et al. Relative quantitation of p53 and MDM2 gene expression in leiomyosarcoma; real-time semiquantitative reverse transcription-polymerase chain reaction [J]. *Cancer Lett*, 2001, **164**(2): 177–188.
- [8] Van Orsouw N J, Dhanda R K, Rines R D, et al. Rapid design of denaturing gradient-based two-dimensional electrophoretic gene mutational scanning tests [J]. *Nucleic Acids Res*, 1998, **26**(10): 2398–2406.
- [9] Wang J X, Zhu X, Tu Q Y, et al. Capture of p53 by electrodes modified with consensus DNA duplexes and amplified voltammetric detection using ferrocene-capped gold nanoparticle/streptavidin conjugates [J]. *Anal Chem*, 2008, **80**(3): 769–774.
- [10] Zhou H J, Xing D, Zhu D B, et al. Rapid and sensitive detection of point mutation by DNA ligase-based electrochemiluminescence assay [J]. *Talanta*, 2009, **78**(4/5): 1253–1258.
- [11] Gupta G, Atanassov P. Electrochemical DNA hybridiza-

- tion assay: enzyme-labeled detection of mutation in p53 gene [J]. *Electroanalysis*, 2011, **23**(7): 1615–1622.
- [12] Farjami E, Clima L, Gothelf K, et al. “Off-on” electrochemical hairpin-DNA-based genosensor for cancer diagnostics [J]. *Anal Chem*, 2011, **83**(5): 1594–1602.
- [13] Raoofa J B, Ojania R, Golabib S M, et al. Preparation of an electrochemical PNA biosensor for detection of target DNA sequence and single nucleotide mutation on p53 tumor suppressor gene corresponding oligonucleotide [J]. *Sensor Actuat B Chem*, 2011, **157**(1): 195–201.
- [14] Han S H, Kim S K, Park K, et al. Detection of mutant p53 using field-effect transistor biosensor [J]. *Anal Chim Acta*, 2010, **665**(1): 79–83.
- [15] Chen C P, Ganguly A, Lu C Y, et al. Ultrasensitive in situ label-free DNA detection using a GaN nanowire-based extended-gate field-effect-transistor sensor [J]. *Anal Chem*, 2011, **83**(6): 1938–1943.
- [16] Jiang T S, Minunni M, Wilson P, et al. Detection of TP53 mutation using a portable surface plasmon resonance DNA-based biosensor [J]. *Biosens Bioelectron*, 2005, **20**(10): 1939–1945.
- [17] Wang Y C, Zhu X, Wu M H, et al. Simultaneous and label-free determination of wild-type and mutant p53 at a single surface plasmon resonance chip preimmobilized with consensus DNA and monoclonal antibody [J]. *Anal Chem*, 2009, **81**(20): 8441–8446.
- [18] Qiu L P, Wu Z S, Shen G L, et al. Highly sensitive and selective bifunctional oligonucleotide probe for homogeneous parallel fluorescence detection of protein and nucleotide sequence [J]. *Anal Chem*, 2011, **83**(8): 3050–3057.
- [19] Wang X Y, Zhang X Y, He P G, et al. Sensitive detection of p53 tumor suppressor gene using an enzyme-based solid-state electrochemiluminescence sensing platform [J]. *Biosens Bioelectron*, 2011, **26**(8): 3608–3613.
- [20] Makmura L, Hamann M, Areopagita A, et al. Development of a sensitive assay to detect reversibly oxidized protein cysteine sulfhydryl groups antioxidant [J]. *Antioxid Redox Sign*, 2001, **3**(6): 1105–1118.
- [21] Park J K, Yee H J, Lee K S, et al. Determination of breath alcohol using a differential-type amperometric biosensor based on alcohol dehydrogenase [J]. *Anal Chim Acta*, 1999, **390**(1/2/3): 83–91.
- [22] Cai H, Lee T M H, Hsing I M. Label-free protein recognition using an aptamer-based impedance measurement assay [J]. *Sensor Actuat B Chem*, 2006, **114**(1): 433–437.
- [23] Li Y, Qi H L, Peng Y G, et al. Electrogenated chemiluminescence aptamer-based method for the determination of thrombin incorporating quenching of tris (2, 2'-bipyridine) ruthenium by ferrocene [J]. *Electrochem Commun*, 2008, **10**(9): 1322–1325.

乙醇脱氢酶共存固相电致化学发光生物传感器对 p53 基因的检测

王晓英¹ 王晓宁² 张相依¹ 陈奋天¹ 朱柯蕙¹ 杨立刚¹ 唐 萌¹

(¹ 东南大学环境医学工程教育部重点实验室, 南京 210009)

(² 西安交通大学第一附属医院血液科, 西安 710061)

摘要:构建乙醇脱氢酶(ADH)共存固相电致化学发光(ECL)生物传感器,对 p53 基因进行检测.多壁碳纳米管、Ru(bpy)₃²⁺及吡咯膜复合物(MWNTs-Ru(bpy)₃²⁺-PPy)修饰电极可有效固载 ssDNA,ssDNA 与纳米金胶(AuNPs)标记的 p53 基因杂交,AuNPs 进而吸附 ADH.将 ADH 参与的专一性的酶促反应与高灵敏的固相 ECL 技术偶联,建立检测 p53 基因的方法.该方法对 p53 野生型序列(wtp53)的检测限为 0.1 pmol/L,对 p53 突变序列(mtp53)和 wtp53 的区分度达 57.1%.应用该方法,MGC-803 胃癌细胞溶解产物中的 wtp53 产生信号强度仅为正常 GES-1 胃粘膜细胞溶解产物中 wtp53 产生信号强度的 61.8%,浓度降低约 59 倍.该方法与传统的 ELISA 法具有较好的互补性,其在癌症早期诊断、临床治疗过程监控等方面具有潜在的应用前景.

关键词:MWNTs-Ru(bpy)₃²⁺ 混聚体;固相电致化学发光;乙醇脱氢酶;p53 野生序列;p53 突变序列;细胞溶解产物

中图分类号:R113